



## A Novel Way of Using Ground Granulated Blast Furnace Slag and Steel Shaving Fibers for Production of Sustainable and Smart Rigid Pavement

L. A. A. Al-Hindawi, A. M. Al-Dahawi, A. S. J. Al-Zuhery\*

Civil Engineering Department, University of Technology Iraq, Baghdad, Iraq

### PAPER INFO

#### Paper history:

Received 13 December 2023

Received in revised form 15 February 2024

Accepted 12 March 2024

#### Keywords:

Rigid Pavement

Waste Materials

Steel Shaving

Mechanical Properties

Self-sensing

### ABSTRACT

Supporting sustainable development, contributing to reducing waste that causes environmental damage, and reducing the use of natural materials are part of preserving the environment and society. This is done by highlighting the manufacture of sustainable concrete pavement of acceptable quality and according to specifications. The authors previously produced a concrete pavement mixture with optimal properties by partially replacing the Portland cement with 55 wt.% of the ground granulated blast furnace slag (GGBFS) in addition to partially replacing the virgin aggregates with 30 wt.% of recycled aggregate from crushed rigid pavement. The goal of this research work is to produce a self-sensing rigid pavement mixture from wastes with high mechanical properties, that is better than regular concrete and less expensive. The new novel mixture has the ability to detect earlier the damages that occur to the concrete pavement so as to obtain a longer life by periodically maintaining the pavement on time. The previous mixture was improved by adding chopped steel shaving fibers with lengths ranging from 20-60 mm in four different volumetric ratios. These are 0.7%, 1%, 1.1%, and 1.2%. The results were compared with those of the basic mixture, and a decrease in workability and slump values were noticed. Moreover, significant improvements in the mechanical properties were obtained. The concrete's resistance to the applied loads increased by increasing the percentage of steel shaving in the mixtures, due to the increasing of cohesion forces within the mixture. The self-sensing capability for the developed mixtures was tested by measuring the changes in the electrical resistance under different types of mechanical loadings. The results showed that the direction of the applied load and the proportion of steel shavings affect the self-sensing properties in terms of the fractional variation in the electrical resistance (FVER, %), which highlights the importance of using steel shavings in producing smart concrete pavements from reused resources more efficiently and highly cost-effectiveness.

doi: 10.5829/ije.2024.37.08b.15

### Graphical Abstract



\*Corresponding Author Email: [ahmed.sh.jeber@uotechnology.edu.iq](mailto:ahmed.sh.jeber@uotechnology.edu.iq) (A. S. J. Al-Zuhery)

Please cite this article as: Al-Hindawi LAA, Al-Dahawi AM, J. Al-Zuhery AS. A Novel Way of Using Ground Granulated Blast Furnace Slag and Steel Shaving Fibers for Production of Sustainable and Smart Rigid Pavement. International Journal of Engineering, Transactions B: Applications. 2024;37(08):1622-38.

## 1. INTRODUCTION

Concrete is a combination of materials that includes cement, aggregates, water, and additives. Sustainability and cost considerations associated with traditional cement-based building materials have prompted the academic and technical community to investigate alternative products, and the current concrete industry faces three significant challenges: diminishing reserves of natural aggregates, increasing carbon due to increased demand for Portland cement, and a corresponding increase in greenhouse gas emissions from the production of Portland cement annually (1). It is often used as the main construction material in many structural applications. Conventional concrete has some weaknesses, including limited ductility and poor tensile strength. Strength is enhanced by the use of reinforcing bars, sometimes supplemented by fibers or polymers (2). Various fiber kinds may be added to concrete mixes to increase certain qualities like as ductility, fracture resistance, tensile strength, and flexural strength (3). The lathe steel fibers can be utilized to reinforce the concrete, but high dosages of fibers leads decreased workability of the freshly mixed concrete (4). However, addition of small quantities of fibers to the concrete improves its mechanical behavior (5). The impact of varying amounts of steel lathe waste on the performance of concrete was investigated by Mansi et al. (6). Incorporating steel lathe waste into the mixture enhanced mechanical attributes like concrete's compressive strength. Nevertheless, when the amount of lathe steel waste is increased, the concrete's workability decreases. Annadurai and Ravichandran (7) investigated the effects of steel lathe waste on the shear, impact, and fracture strengths of concrete. The output of that research showed that the steel lathe waste significantly slows the spread of cracks. The impact of varying amounts of steel lathe scrap on the performance of concrete was previously examined (6). The results showed that the mechanical qualities including compression strength were enhanced when steel lathe waste was added to concrete. The flexural behavior of concrete made from waste lathe fiber was studied by Akshaya et al. (8). The researchers stated that addition of lathe fibers to concrete improves its flexural strength and reduces cracking length. The other reasons for using recycled materials are that the cost of constructing rigid pavements continues to rise, and there is an increasing demand for materials that can improve the mechanical and electrical properties of the rigid pavement (9). The manufacturing of smart concrete pavement that has acceptable mechanical properties is very important for early detection of damage and, therefore, extending the life of the pavement and enhancing its durability and, thus, reducing the rehabilitation and maintenance costs (10-13). In most studies of cement-based self-sensing materials, electrically conductive filler(s) is/are

responsible for the initiation of electrical networks within cement-based matrices (14-17).

In the present work, to manufacture a self-sensing concrete pavement, information about the strength, displacement, or damage of crack structures is based on the change of electrical resistance (13, 18). The primary determinant of electrical conductivity of concrete is the conductive ability of the filler. Currently, conductive fillers are mainly based on metals (19). The incorporation of chopped steel shaving fibers into concrete has the potential to substantially decrease its electrical resistivity, owing to the elevated electrical conductivity of steel. The presence of steel shavings in the concrete matrix facilitates the conduction of electrical current by serving as conductive pathways (20). The sustainable concrete in this research consists of materials that affect both mechanical and electrical properties, as the use of crushed concrete aggregates as a partial substitute for natural aggregates can have contradictory effects on the strength. It depends on factors such as the classification of the crushed concrete aggregate, the gradation of the aggregate, and the overall composition of the concrete mix. Moreover, ground granulated blast furnace slag (GGBFS) is an iron and steel industry byproduct, which the Portland cement is partially supplanted with it to produce the concrete pavement mixtures in the present work. As a consequence, addition of GGBFS may affect the concrete strength and decrease its electrical resistivity (21). When comparing the methodology of this research with some previous works (22, 23), it becomes clear that by using lower percentages of chopped steel shaving fibers by volume of the mixtures (0.7, 1, 1.1, and 1.2%), high load resistance and good cohesion of the concrete are obtained without a negative impact on workability and slump test. This were obtained with the utilization of optimal addition ratio and appropriate lengths of steel shaving fibers. Briefly, in the present work, a novel, sustainable (made with moderately high percentages of waste materials (RCA, GGBFS and steel shaving fibers)) and smart concrete pavement mixture is suggested to fill the gap left within the literatures.

## 2. LABORATORY EXPERIMENT PROGRAM

### 2. 1. Materials Used and Mixes

**2. 1. 1. Cement** In this paper, sulfate-resistant Portland cement CEM I 42.5 R- SR3.5, was utilized. The chemical and physical properties of the cement used are summarized in Table 1.

**2. 1. 2. Fine Aggregates** Washed sand free of salts and impurities was used, and it does not contain more than 4% separable materials. It is a red sand type and it is present Al-Ukhaidir area in Karbala. The sand gradations have been checked according to AASHTO T27 (24) as

stated in Table 2. and presented in Figure 1. This gradation of the size of aggregate granules produces a high-quality concrete mixture and fills the voids between the coarse particles, as well as has an effect on the workability of the fresh concrete (25).

**2. 1. 3. Coarse Aggregates** Two types of aggregates were used, the first type was natural aggregates it was sourced Al-Nebai area in Salahaldeen Governorate, and the second type was recycled aggregates. It was sourced from a demolished rigid pavement and converted into coarse aggregates of different sizes using a crusher. Coarse aggregates of both types are washed with water and cleaned of impurities and dust that affect the cohesion of concrete. Coarse aggregates are classified into specific grades according to Iraqi specification (26), depending on AASHTO T27 (24) as given in Table 3. and

**TABLE 1.** Chemical and physical properties of the Portland cement used

Characteristic	Value
<b>Chemical properties</b>	
Loss on flicker	3.56
Insoluble materials	0.50
SO <sub>3</sub>	2.37
C <sub>3</sub> S	2.49
MgO	1.70
Chloride quantity	0.03
<b>Physical properties</b>	
Finesse (m <sup>2</sup> /kg)	344
Primate time(min)	150
Final time (hours)	3:18
Hardness (mm)	0.29
<b>Compressive strength (MPa)</b>	
2 days	23.9
28 days	48.2

**TABLE 2.** Fine aggregates gradation according to AASHTO T27

% Passing by weight		
Upper limit	Chosen gradation	Lower limit
100	100	100
100	95.87	95
80	64.37	45
30	21.96	12
10	3.95	2
3	1.71	0

exhibited in Figure 2, to obtain the largest amount of inlet between the grades of aggregates, and this, in turn, leads to an increase in the strength of the concrete (27).

**2. 1. 4. Ground Granulated Blast Furnace Slag (GGBFS)**

It is a byproduct of iron production and when mixed with concrete it may enhance its strength and durability. This substance is created by heating iron ore, limestone, and coke to around 1500 °C. The procedure takes place in a blast furnace. GGBFS does not form straightforwardly. Molten slag and molten iron are byproducts of iron production. The molten slag is made up of alumina, silica, and a few oxides. After cooling, the

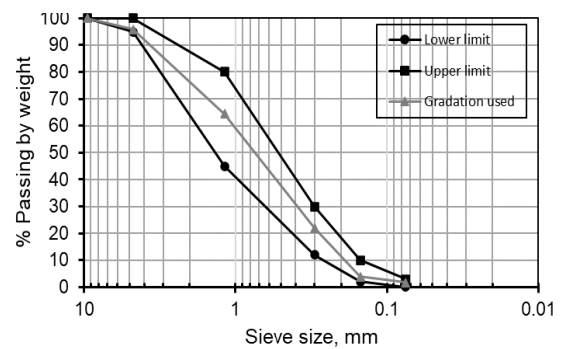


**Figure 1.** Gradation limits and the selected gradation of the fine aggregates used

**TABLE 3.** Coarse aggregate gradations according to SCRBR10 (28) and AASHTO T27 (24)

% Passing by weight		
Upper limit	Chosen gradation	Lower limit
100	100	100
100	99	90
70	70	35
30	30	10
5	1	0
1	1	0

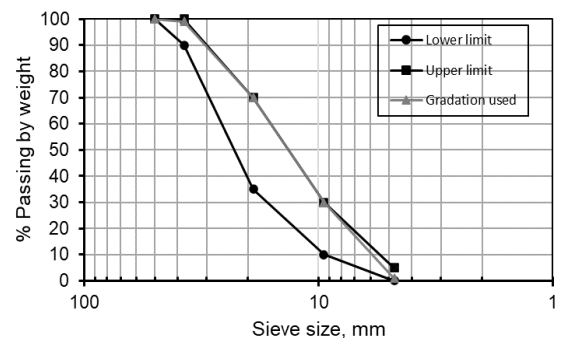


**Figure 2.** Gradation limits and the selected gradation of the coarse aggregates used

slag is granulated. It is authorized to travel through high-pressure water for this purpose. This causes the particles to quench, resulting in granules with diameters smaller than 5mm. The presence of the major oxides are typically found to be within the following ranges: MgO (0-21 %), Al<sub>2</sub>O<sub>3</sub> (5-33 %), SiO<sub>2</sub> (27-42 %) and CaO (30-50 %) (29). These are the minerals contained in the majority of cementitious compounds. The particles are then dried and processed in a revolving ball mill to generate a fine powder known as ground granulated blast furnace slag.

**2.1.5. Steel Shaving Fibers** A waste of lathe iron was used to study the direct impact on concrete. The recycled steel shaving obtained from the lathe machine was spiral in form. Before usage, the recycled steel is cut into specified pieces. Figure 3 exhibits the steel shaving fibers production and uses in concrete. The dimensions of the steel shaving fibers used were 2mm wide and 0.1mm thick, and the length was controlled between 20 to 60 mm. Each lathe produces approximately 2-3 kg of steel shaving refuse filaments per eight-hour workday. Steel shaving fibers were used in the present work to decrease the electrical resistivity and enhance the mechanical properties of the produced mixtures.

**2.2. Mixing Procedures** The materials were mixed in three stages: the first stage was the dry mixing, which

includes the dry mixing of the fine and coarse aggregates both 70 wt.% of natural aggregates and 30 wt.% of recycled crushed concrete aggregates were blended in the mixer in addition to the 45 wt.% of cementitious materials of Portland cement and 55 wt.% of GGBFS. All these components were dryly mixed for five minutes. The second stage starts at the moment when water is added to the ingredients. With the aid of the addition of the high range water reducing admixture (HRWRA) to facilitate the mixing process and get a well-mixed concrete, the wet mixing process continues for about ten additional minutes. These two stages of mixing were performed according to the steps suggested by a previous work of the authors (30). Different proportions of steel shaving fibers by volume of mixtures (0.7%, 1%, 1.1%, 1.2%) were slowly distributed and mixed with the fresh concrete during the third phase for an additional five minutes to avoid balling and agglomerating of steel shavings. It was noted that the addition of steel shaving fibers negatively affects workability, especially at a dose of 1.2% vol. After completing the mixing process, the mixtures were molded and vibrated for 20 seconds, and finally covered with plastic sheets and kept at room temperature for 24 h after molding. The curing stage of the specimens is started after the demolding process by immersing the specimens in water until they reach the age at which the test is performed.



(a) Lathe machine



(b) Waste steel fibers after cutting



(c) The use of waste steel fibers in concrete

**Figure 3.** The steel shaving fibers production and use in concrete

**2.3. Types of the Experimental Tests** The tests that were carried out in the present research include the tests on the fresh concrete in terms of slump value, as well as the tests on the hardened concrete, which cover the compressive, indirect tensile and flexural tests. Moreover, the piezoresistive behavior of the specimens under the above loading scenarios were investigated (Figure 4).

**2.3.1. Slump Test Results** The results of the slump test are shown in Figure 5. It was observed that the high percentage of utilization of steel shavings in the mixture leads to a decrease in the amount of slump. The

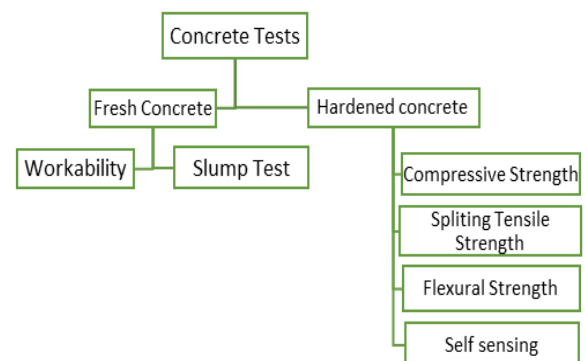


**Figure 4.** Types of performed tests

reason may be attributed to the enhanced bonding between the concrete compounds, specifically the concrete reinforcement (4). The increase in the percentage of steel shaving with lengths (20-60mm) makes the ingredients difficult to mix because it reduces workability as a result of the cohesion that occurs between these parts inside the mixer.

**2.3.2. Experimental Procedures** Three kinds of tests were executed to determine the mechanical properties of the concrete acquired by adding steel shaving after a curing period of 7, 28, and 56 days. The tests were compression for the cubic specimens, indirect tension for the cylindrical specimens and flexure for the prismatic specimens. During the loading process of these specimens up to failure, the electrical resistance values were recorded to capture the self-sensing behavior of the produced mixtures. Three samples of each mixture were tested and the results were averaged. The compressive strength was tested using  $100 \times 100 \times 100 \text{mm}^3$  cubic specimens. Cylindrical molds with a diameter of 100mm and a height of 200mm were utilized to manufacture the specimens that were loaded under indirect tension. The flexural test was carried out to prismatic specimens of  $100 \times 100 \times 400 \text{mm}^3$ . The values of the tests were obtained as shown in Table 4. The specimens were tested at a loading speed of 0.2 MPa/sec for compression test BS-EN-12390-6, (31), 1.0 MPa/min for splitting tension test

(32), and 1.0 MPa/min for flexural third point test (33) until failure.

### 3. RESULTS AND DISCUSSION

**3.1. Compressive Strength** Table 5 shows the results obtained from the compression test of concrete cubes containing steel shaving at four different proportions (0.7, 1, 1.1, and 1.2). It was noted that the samples containing steel shaving have a higher compressive strength than the control mix (R30S1.2), and the amount of strength is increased with the increase in the percentage of steel shaving fibers. Figure 6 shows the direct relationship between the percentage of steel shaving fibers and the compressive strength for the three curing ages 7, 28, and 56 days.

The compressive strength of concrete samples is significantly influenced by both the curing period (34) and the proportion of steel shavings incorporated into the concrete mixtures. A higher percentage of steel shavings results in a notable increase in the compressive strength, with enhancements ranging between 19% and 21% when compared to the base mixture (R30S1.2) without steel shavings. The concrete constituents and densification can enhance the overall compactness of the concrete, making it more resistant to various types of stresses (34).

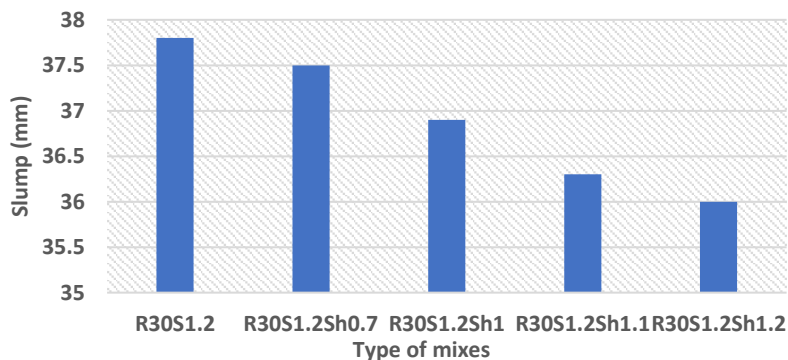


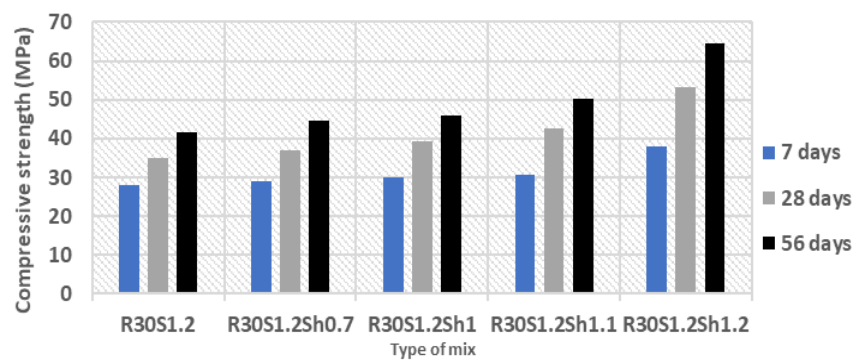
Figure 5. Slump test results

TABLE 4. Proportions of materials used in all mixes

Mixes [Mix code R (recycled concrete aggregate), S(slag), Sh (steel shaving).	% GGBFS/ Cement	% GGBFS	% Vol. Steel shaving fibres	Steel shaving fibers (Kg/m <sup>3</sup> )	% Cement	% RCA	% FA	% NCA	% w/c	% HRWRA
R30S1.2	1.2	55	0	0	45	30	100	70	0.35	0.3
R30S1.2Sh0.7	1.2	55	0.7	15.5	45	30	100	70	0.35	0.3
R30S1.2Sh1	1.2	55	1.0	22.15	45	30	100	70	0.35	0.3
R30S1.2Sh1.1	1.2	55	1.1	24.36	45	30	100	70	0.35	0.3
R30S1.2Sh1.2	1.2	55	1.2	26.58	45	30	100	70	0.35	0.3

**TABLE 5.** The results of strength for five mixes

Mix type	Mixture strength (MPa)						
	Compressive			Indirect tensile			Flexural
	Mixture age (days)						
	7	28	56	7	28	56	56
R30S1.2	28.01	35.07	41.76	2.24	3.03	3.59	8.87
R30S1.2Sh0.7	28.95	37.11	44.52	2.44	3.25	3.88	9.40
R30S1.2Sh1	29.98	39.45	45.89	2.67	3.55	4.17	9.40
R30S1.2Sh1.1	30.74	42.69	50.11	2.88	3.93	4.43	11.68
R30S1.2Sh1.2	37.86	53.33	64.60	3.29	4.57	4.95	13.08

**Figure 6.** Compressive strength of the plain and modified mixtures at different curing ages

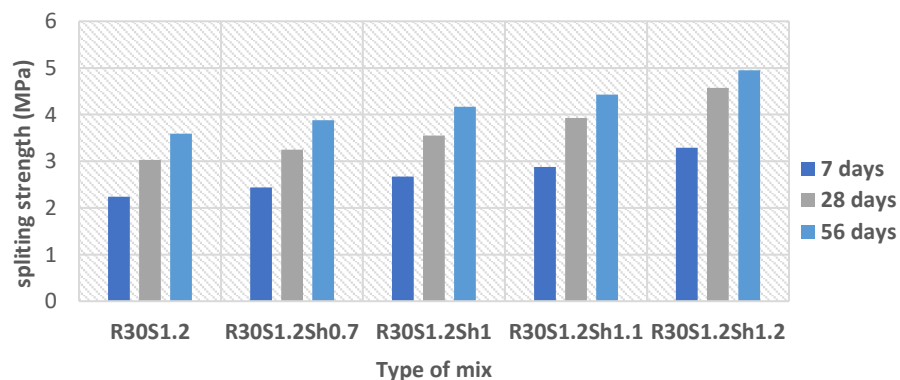
**3. 2. Splitting Tensile Strength** The purpose of incorporating steel scrap into concrete is often to achieve a ductile failure response, as plain concrete tends to exhibit brittle failure characteristics under tension. The impact of using discarded steel scrap on tensile behavior is prominently illustrated in Figure 7.

By adding waste steel to the control mix with curing age of 7, 28 and 56 days, the strength increases in the ranges of 8% - 19%.

The results exhibit an improvement in the elastic behavior capacity of the specimens. As the waste steel-

to-volume ratio increased, the strength and ductility of the material also increased to some extent. In a previous study, the results showed that lathe residues significantly increase the strength, ductility and ultimate stress of concrete (35).

**3. 3. Flexural Strength** Table 5 gives the result values that reflect the effect of adding lathe waste pieces on the flexural strength of concrete at 56 days age. The results indicate that the flexural strength increases proportionally when the steel shaving fibers are added to

**Figure 7.** Splitting tensile strength of different mixes with different curing ages



the mixture. In their research on synthetic fiber-reinforced concrete, Balamuralikrishnan and Saravanan (36) observed an increase in post-cracking energy absorption capacity and ductility, as well as a significant increase in both flexural fatigue strength and toughness compared to conventional concrete. The flexural strength of concrete is achieved by integrating straight and corrugated steel and hook. By comparing the mixture (R30S1.2) with the four mixtures containing steel shaving, an enhancement in the flexural strength between 6%-46% was obtained. This enhancement is proportional to the amount of steel shaving fibers.

Figure 8 illustrates the increasing in the flexural strength with the rising in the percentage of steel shaving, as the corrugated and irregular shape of the lathe iron sheets provide higher strength for cohesion and bending after shedding the load compared to the plain mix, as stated by Junaid et al. (35).

**3. 4. Electrical Resistivity Measurement** The electrical resistance was checked at the same time as the applied load recorded. A DC source meter was used to measure the electrical resistance. Three samples of each type of mixtures were examined by implanting copper electrodes in the fresh concrete of each sample (Figure 9).

During the mechanical test, DC electrical resistance was measured along the stress axis using binary electrodes, which previously embedded in the fresh concrete. To achieve reliable results, a DC source meter was utilized. A wooden board was constructed between the loading device and the samples to avoid electrical conduction that might affect the accuracy of the data. Figure 9 shows the entire pressure testing and self-sensing apparatus. A data acquisition system was used to record the electrical resistance (Figure 8b). In addition, the electrical resistance measurements were obtained using a DC source meter, as shown in Figure 8c. As a result of the above, the electrical resistivity data are generated, which are then converted to fractional variation in electrical resistivity (FVER, %) using Equation 1.

$$\text{FVER} \left( \frac{\Delta\rho}{\rho_0} \right) \% = \left( \frac{\rho_t - \rho_0}{\rho_0} \right) \times 100 \% \quad (1)$$

where FVER,  $\rho_0$  and  $\rho_t$  are the fractional variation in electrical resistivity, initial electrical resistivity and electrical resistivity when the specimen is under loading respectively. Figure 10. presents the geometrical dimensions of the specimens and copper plates. The methodologies and electrode types used in this approach are based on literature (10, 34).

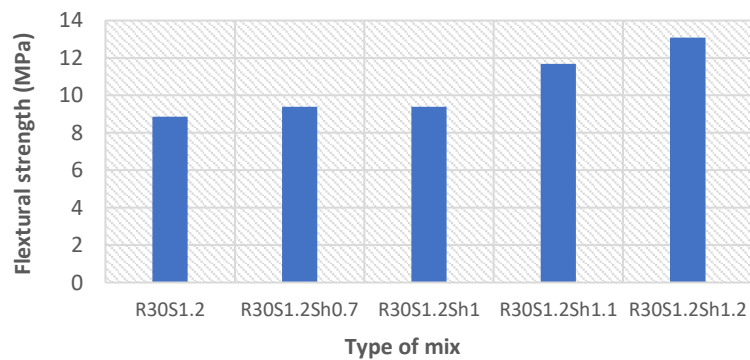


**Figure 8.** Flexural strength of the produced mixtures after 56 days of curing

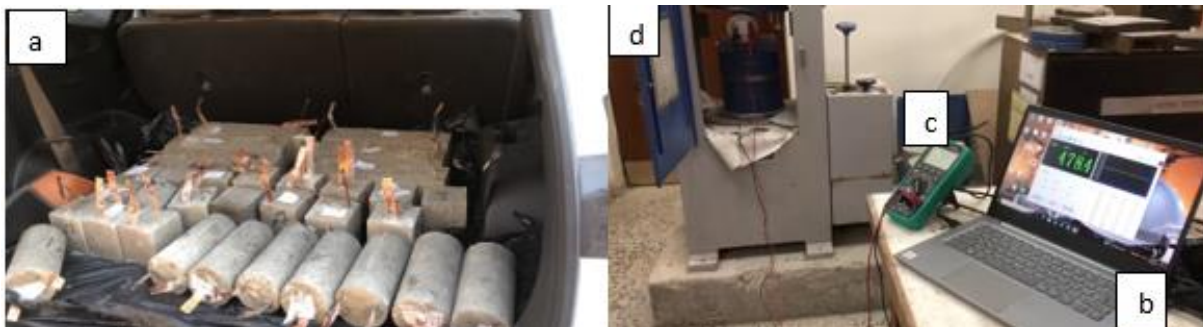


**Figure 9.** Self-sensing setup: (a) Concrete specimens with embedded electrodes, (b) Data acquisition system for the electrical resistivity measurement, (c) DC electrical source meter, (d) Compressive strength machine

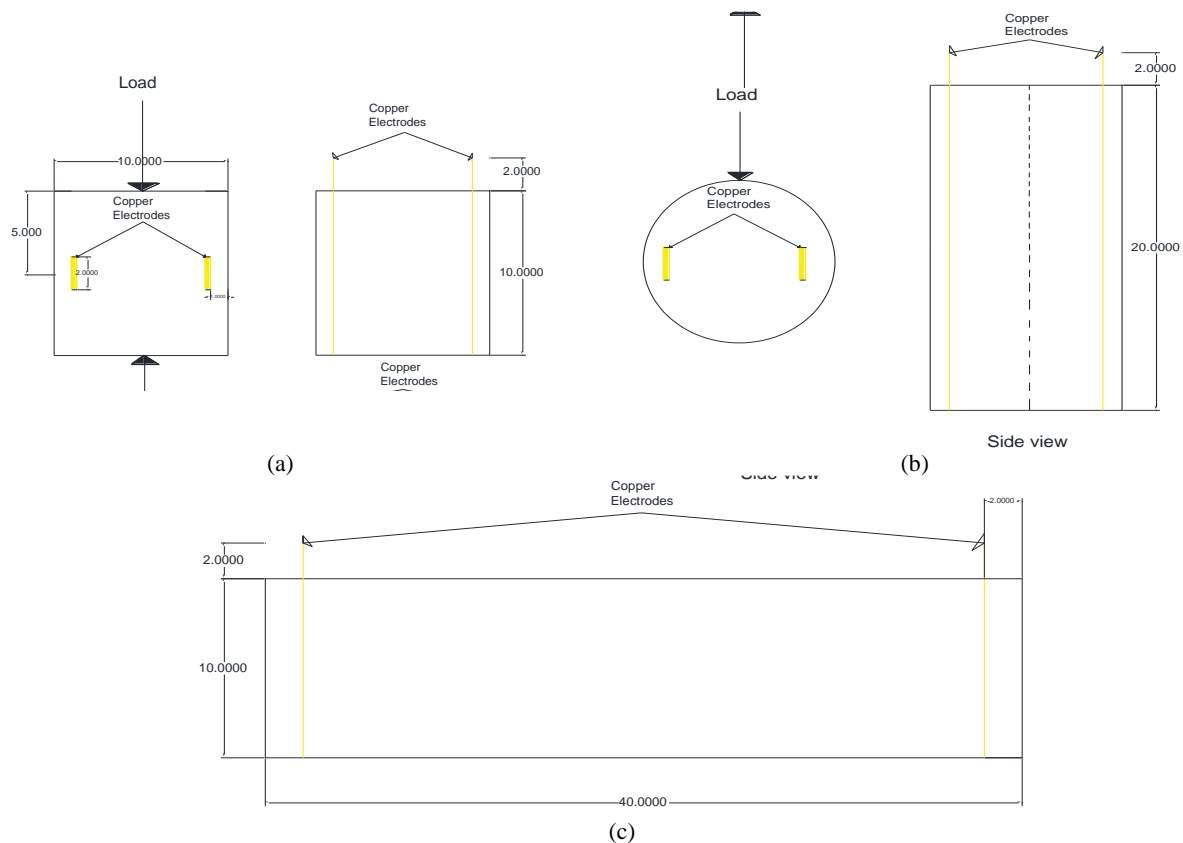


**Figure 10.** The geometrical dimensions and electrode positions of the (a) cubic, (b) cylindrical and (c) prismatic specimens (all dimensions are in centimeters)

### 3. 5. Ultrasonic Pulse Velocity Test (UPV)

Ultrasonic testing devices can identify cracks and voids in concrete and monitor its strength. The device consists of a display unit, two power adapters (54 kHz), two 1.5 m BNC cables, a connector, a calibration rod, a battery charger with USB cable, and 4 AA batteries (LR6).

Ultrasound velocity was measured for a 28-day-old cubic samples of 10cm<sup>3</sup> cubic specimens (11). The electric transducer is in contact with one area of the concrete surface, and the longitudinal pressure wave pulses are generated by the transducer. The second transducer, located at a distance L from the source of the pulses, receives these pulses and converts them into electrical energy. After penetrating the concrete, the transducer sends out its electrical signals. The electronic measurement of time spent in transit is denoted by the letter "T." Dividing L by T, the pulse frequency, V can be determined. Figure 11 presents the Proceq Pundit Lab method. After adjusting the instrument settings using the manufacturer's instructions, three samples were lubricated to ensure smooth operation during the test. The test was performed by determining the time taken for the ultrasonic pulses to pass into the concrete.

Sample quality and mix homogeneity can be determined, using approved standards such as BS. A low speed indicates that the concrete mixture contains voids

and cracks, while a high speed indicates that the material quality and consistency are high and the materials composition are highly packed (37). To ensure more accurate results, the water-saturated samples were dried at 60 °C for 24 hours because the pulse speed in the wet samples was five percent higher than the speed in the dry concrete, and then the samples were lubricated on the opposite sides on which the poles were placed. Ultrasound propagates in a straight path between the two ends of the sample, as specified in the standard were determined (38).

### 4. DESCRIPTION OF STRENGTH RESULTS

Steel shaving fibers, a byproduct of the lathe machine, are waste material beneficial to sustainable concrete product. The improvement of concrete strength increases by increasing steel shaving content in all concrete mixes, as a 1.2% of steel shavings as a volumetric ratio of a sample gives the higher strength amount in the present work. The reason is due to the results of cohesion that occurs between the matrix parts inside the mixtures, as illustrated in Figure 12.

Through previous studies, it was found that the use of steel fibers in different proportions in the concrete



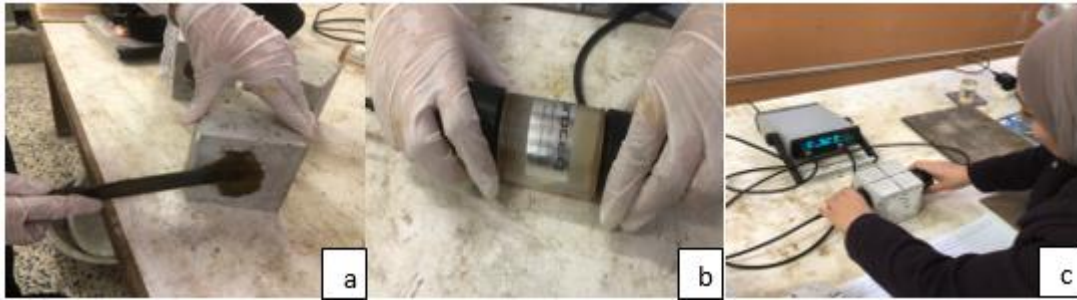


**Figure 11.** Ultrasonic Pulse Velocity test: (a) Lubrication surfaces of the cube, (b) UPV calibration, and (c) Ultrasonic test of a specimen



**Figure 12.** Concrete specimens after failure

mixture affects the strength (39). It was concluded that the use of 1% steel fibers with a length of 30-50 mm led to a decrease in a slump from 19 cm in the base mix to 17 cm. As for the compressive strength, it increased by 11% compared to the base mixture at the age of 28 days. As for Aksoylu et al. (40), they also used steel fibers but with short lengths and different proportions. One percent steel fibers by volume in their work led to a decrease in workability and slump. Concerning the alteration of normalized splitting tensile strength, Çelik et al. (22), demonstrated a 70% augmentation in their research, whereas Shewalul (41) observed a decline of 13%. Accordingly, it can be stated that the amount of slump and workability do not depend on an increase in the percentage of steel only, but also on the shape and size of the additive, as an increase in these percentages sometimes gives counterproductive results. Moreover, if there are no balling cases in the produced mixtures, the compressive strength can be enhanced significantly with the addition of reinforced fibers. The linking bonds between the cement hydration products and fibers increases the elasticity, ductility, and durability of concrete. The irregular nature of lathe waste pieces is also an essential property that contributes to their adhesion, as they adhere effectively to cement and aggregate.

## 5. UPV TEST RESULTS

The pulse velocity checked by ultrasonic test instrument for concrete cubes for all concrete mix types are shown

in Table 6 and figuratively presented in Figure 13. The sample size affects the exactitude of the UPV test results. A previous study by Prasad et al, (42) verified this fact, indicating that the specimen dimension would be under 50 mm and not exceeding 100 mm as the pulse is both large or small at short distances. As a consequence, discrepancies in the values of the test findings are possible. To establish the quality of the mixes, the test results were compared to British Standards (BS). The BS Standards categorize ultrasonic pulse velocity across samples as extremely bad, weak, questionable, acceptable, or exceptional (43), as shown in Table 7. Figure 8 shows that the UPV values of the mix R30S1.2Sh1.1 reinforced with steel shaving of 1.1 vol.% has the highest pulse speed (4410 m/s), while the mix with steel proportion (0.7, 1, 1.2%) showed a significant decrease in pulse speed, even when compared to the plain mix, which reached 4206 m/s. All combinations, however, may be considered excellent homogenous mixtures. Furthermore, the difference in average pulse

**TABLE 6.** UPV test results

Type of mix	Time (µsecond)	Velocity (m/s)	Condition
R30S1.2	21.9	4110	Good
R30S1.2Sh0.7	20.9	4306	Good
R30S1.2Sh1	22.4	4318	Good
R30S1.2Sh1.1	21.2	4410	Good
R30S1.2Sh1.2	21.4	4408	Good

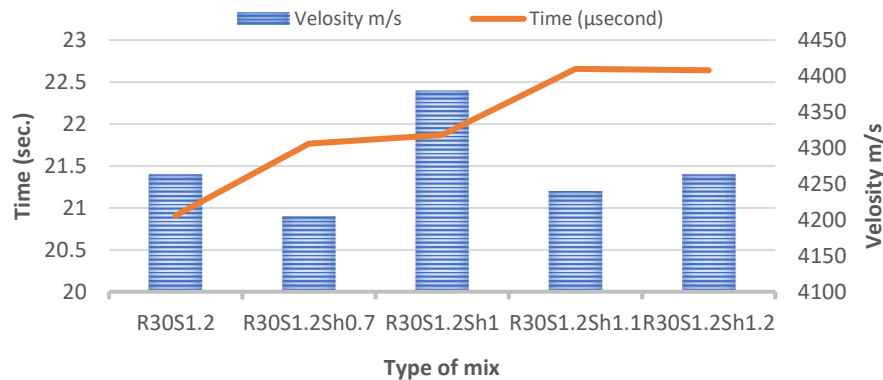


Figure 13. Pulse transfer velocity results

TABLE 7. Pulse velocity ranges for concrete (43)

Pulse velocity (m/sec)	General conditions
Above 4570	Excellent
3660 – 4570	Good
3050 – 3660	Questionable
2130 – 3050	Poor
Below 2130	Very poor

speeds caused by the presence of hybrid fillers provided the impression that the electrically conductive materials impacted the homogeneity and strength of the mix, which is in line with the results obtained by Abdullah et al. (16). They demonstrated that the kinds of components and their amounts in the cement-based combination influence pulse speed.

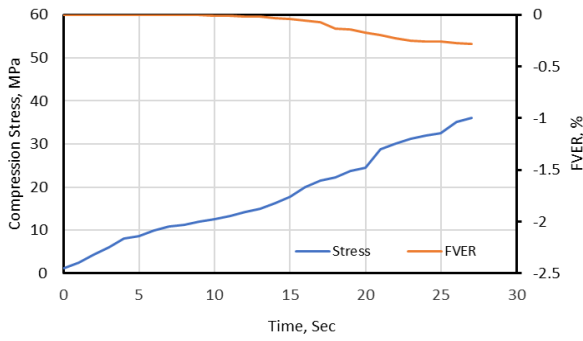
## 6. SELF-SENSING BEHAVIOUR OF SPECIMENS UNDER LOAD APPLICATION

Electrical resistivity is indicated by how well the material conducts electricity within concrete. The benefit of determining the fractional variation in the electrical resistance (FVER, %) is in the early detection of cracks that occur in rigid pavement and their maintenance at the lowest cost before these cracks get worse and become a major problem. As a result, the upkeep of these necessitates the highest expenses. In this research, the produced sustainable concrete pavement consists of recycled aggregates, GGBFS, and steel shaving, as each of these three materials affects the piezoresistive behavior of the produced mixtures. The produced specimens, as mentioned before, were tested under three loading scenarios; compression, indirect tension and bending. Electrical resistance was measured simultaneously with mechanical tests each one second.

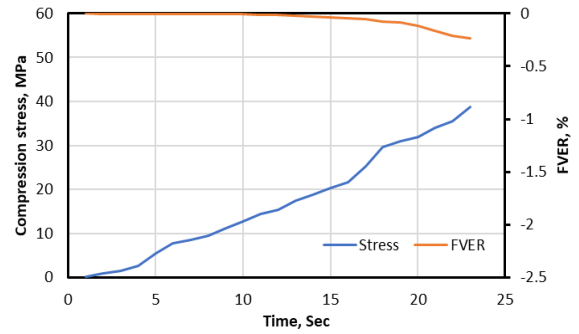
### 6. 1. Behavior of Self-sensing Under Uniaxial Compression Test

Figure 14 illustrates the correlation among the self-sensing behavior of mixtures, as indicated by the Fractional Variation in Electrical Resistance (FVER, %), and time under uniaxial compression loads for all of the four proportions of steel shaving (0.7, 1, 1.1, and 1.2 vol.%) that utilized within the mixtures. The piezoelectric test was carried out two times depending on the direction of the load application relative to the direction of the measurement of the electrical resistance (parallel and perpendicular). The research demonstrates the self-sensing capabilities of cubic specimens composed of various mixtures when subjected to uniaxial compressive loading after a 28-day curing period. Figure 14. presents the compression stress and FVER changes along the time of test performing when the direction of the applied load was parallel to the direction of the electrical resistance measurement. The piezoresistive behavior of the mixtures containing different dosages of steel shaving fibers exhibits similar pattern. There were small differences between the mixtures in terms of FVER. It can be seen clearly that the FVER at 1.1 vol.% steel shaving registered the higher change comparing with other percentages. This can be attributed to the effectiveness of the electrical network formed at this ratio of fibers, which led to a greater change in the electrical resistance when the samples were subjected to compressive loads. Moreover, the increase in FVER may be due to the cohesion exhibited by concrete particles and the reduction of existing voids, as well as the presence of steel in a helical form that prevents further formation of micro-cracks and thus makes the specimens coherent even after failure. That is, the presence of a good medium that transmits electrical ions and thus more changes can be obtained (40).

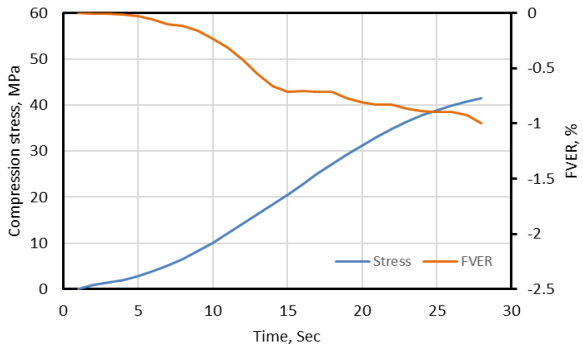
Figure 15 exhibits the self-sensing behavior of the produced mixtures when the direction of the applied load was perpendicular to the direction of the electrical resistance (ER) measurements. According to this setup, it



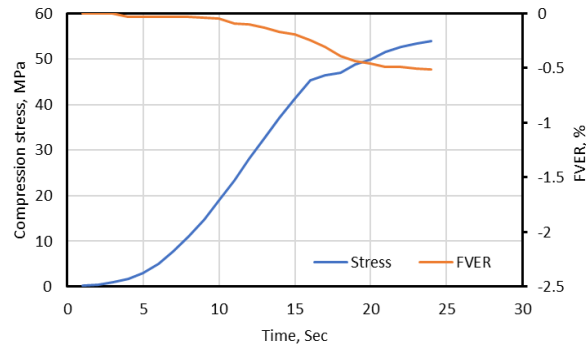
(a) 0.7 % vol. steel shaving



(b) 1.0 % vol. steel shaving

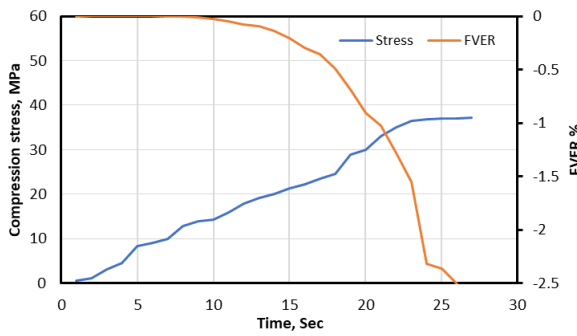


(c) 1.1 % vol. steel shaving

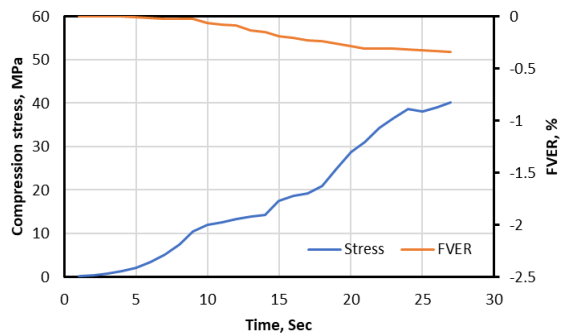


(d) 1.2 % vol. steel shaving

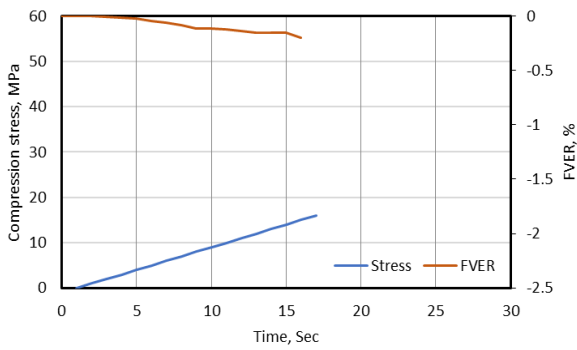
**Figure 14.** Piezoresistive behavior of cubic specimens with different percentages of steel shavings under uniaxial compression load with load application parallel to the ER measurement



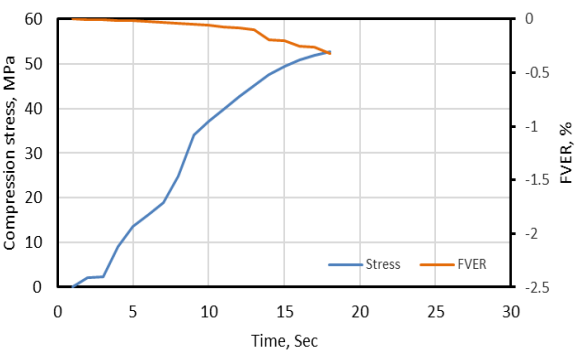
(a) 0.7 % vol. steel shaving



(b) 1.0 % vol. steel shaving



(c) 1.1 % vol. steel shaving



(d) 1.2 % vol. steel shaving

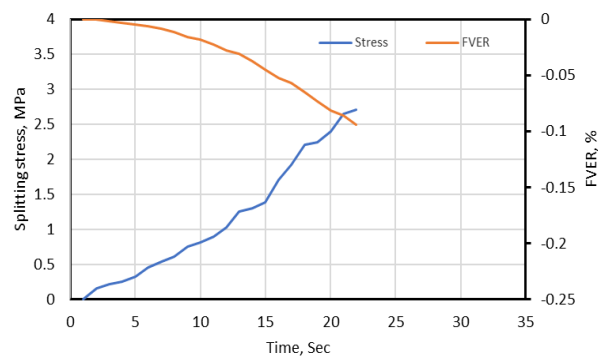
**Figure 15.** Piezoresistive behavior of cubic specimens with different percentages of steel shavings under uniaxial compression load with load application perpendicular to the ER measurement

was noted that the mixture containing 0.7 vol.% steel shaving reached to FVER of 2.5%, performed better than other mixtures in spite of the low percentage of fiber used in it. The high FVER obtained in this mixture under the uniaxial compression loads may be attributed to the well dispersed process of the steel shaving fiber that leads to the creation of a good electrical network within the concrete matrix that highly can self-sense the applied load on it (10, 17, 44, 45).

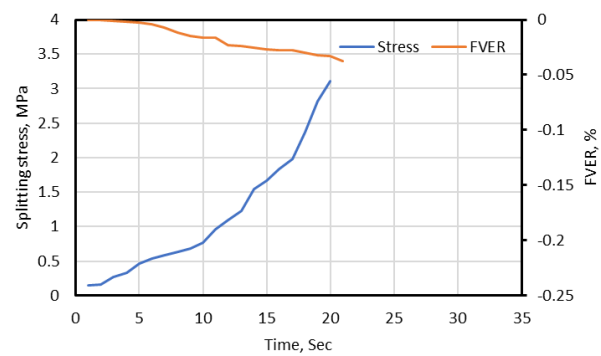
## 6. 2. Behavior of Self-sensing Under Splitting Tensile Test

As presented in Figure 16, the self-sensing characteristics of concrete mixture samples change with the proportion of steel shaving amount. Through the use of reinforced concrete in this work, the splitting tensile strength of the cylindrical specimens under the applied load can be determined, as the concrete gradually cracks when the load is applied until it reaches the failure stage. As a result, the electrical resistance was measured to early capture the micro crack happening in the concrete and enable maintenance of initial cracks in the real-world pavement structures before they reach the deterioration stage. Figure 16 displays the self-sensing behavior of the cylindrical specimens under indirect tension loads where the direction of the applied load is parallel to the ER measurement via the copper electrodes embedded in the concrete. As previously mentioned in

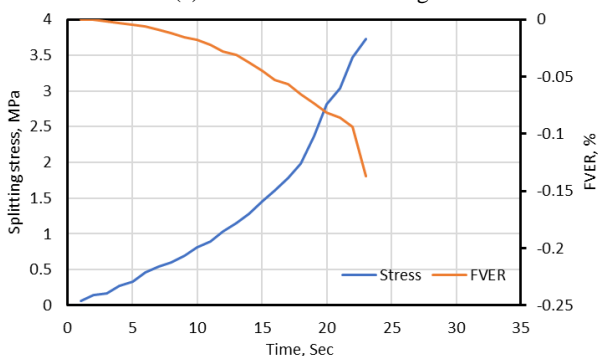
section 6.1, the self-sensing capability is measured by determining the fractional variation in electrical resistance FVER for all mixes. It was noted that all types of mixtures reinforced with different amounts of steel shaving fibers well behaved in terms of FVER with clear superiority of the mixture reinforced with the highest amount of steel shavings (i.e. the mix that contains 1.2 vol. %), which reached to FVER of 0.22%. This may be explained due to the obvious effect of the reinforcing fibers on the self-sensing behavior of the mixtures when they loaded with the splitting loads. Moreover, it can be concluded that the electrical resistivity of all types of the loaded mixtures were decreased because the ER was measured parallel to the applied load, which indicates that the electrodes come closer together when the indirect tension load is applied, while measuring the electrical resistance as shown at the beginning of this section. As for Figure 17, the split load is applied in a direction perpendicular to the ER measurement. It was observed that the resulting FVER for mixtures containing (0.7, 1.1 vol. %) steel shaving fibers had very small values, but the mixture that contains 1 vol. % steel fibers reached to FVER of 0.48% at the end of the splitting test of the cylinders. The highest amount of the steel shaving fibers and also irregular behavior appears in mix 1.2%, where the FVER of 9%, again proved their self-sensing superiority, although there is self-sensing in the rest of



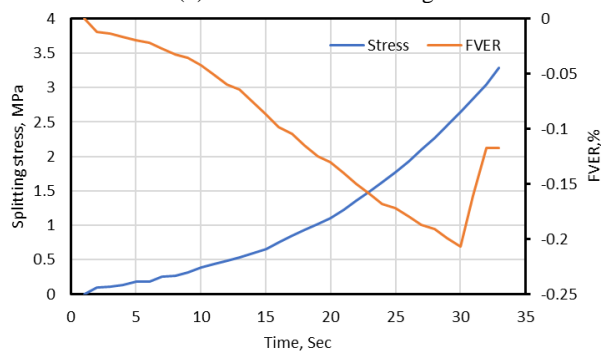
(a) 0.7 % vol. steel shaving



(b) 1.0 % vol. steel shaving



(c) 1.1 % vol. steel shaving



(d) 1.2 % vol. steel shaving

**Figure 16.** Piezoresistive behavior of cylindrical specimens with different percentages of steel shavings under splitting load with load application parallel to the ER measurement

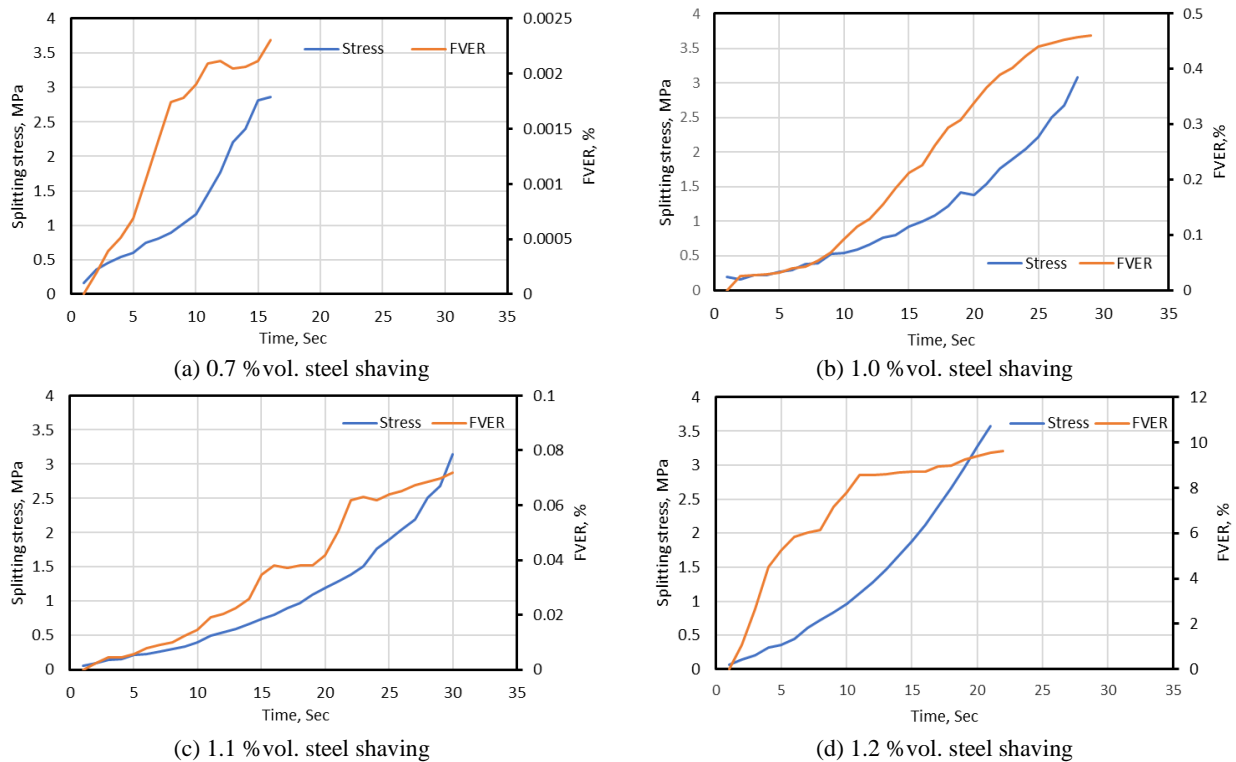


**Figure 17.** Piezoresistive behavior of cylindrical specimens with different percentages of steel shavings under splitting load with load application perpendicularly to the ER measurement

the mixtures. As it can be noticed, the FVER raises with the increasing of the splitting loads in all mixtures. This can be explained by the electrodes being farther away from each other with the progression of the split load applications until failure. Moreover, the ER changes as a result of the concrete particles sliding, their position changed, the electrodes moved apart, and cracks occurred. All of these reasons lead to an interruption in the network that transports ions, thus increasing electrical resistance. From this, it is useful to utilize steel shaving reinforcement within the mixtures, and the use of high percentages are better than low percentages, as the FVER obtained, which is the index of the self-sensing phenomenon are higher. In addition, the steel shaving fibers show good behavior in terms of the cohesion of concrete and controlling the microcracks that occur during the load application (10, 11, 16, 17, 45).

### 6. 3. Behavior of Self-sensing of the Prismatic Samples under Flexural Loads

The flexural test is important to determine the ability of the rigid pavement to bend. The test was carried out using four-point flexural test according to ASTM C78 (33). The capacity of the loading machine is 200 kN, and the prismatic specimens were loaded at a loading rate of 1.0 MPa/min, with a computer connected to the loading machine to record the flexural load and mid-span displacement each second until failure, simultaneously with the recording of the

electrical resistance via the embedded electrodes as shown in Figure 18. Electrical resistance values were measured and registered during the process of applying the flexural loads on the specimens with the aid of a DC source meter each one second. After that, the FVER was determined to quantify the self-sensing ability of the prismatic specimens against the applied loads and the resulted mid-span displacement. The electrodes were positioned at a distance of 25 mm from the edge of the prismatic specimens, specifically at the positions of the support points, to avoid the earlier failure of the prisms, since the electrodes create weak points that lead to crack propagation under loading (Figure 18 b).

The self-sensing results obtained during the four-point bending in terms of FVER are presented in Figure 19. The figure exhibits the self-sensing behavior that may be divided into three segments, each showing variations in flexural stress-deformation plots. The first phase encompasses the region from the onset of flexural loading until the development of the first fracture when the flexural stress-deformation relationship remains linear (elastic stage). The second stage starts after the first cracking and involves a simultaneous process of deflection-hardening along with the occurrence of several microcracks. The third "part" may be regarded as the region of deflection-softening, characterized by an abrupt decrease in the ability to bear flexural loads, caused by the process of identifying the specific location



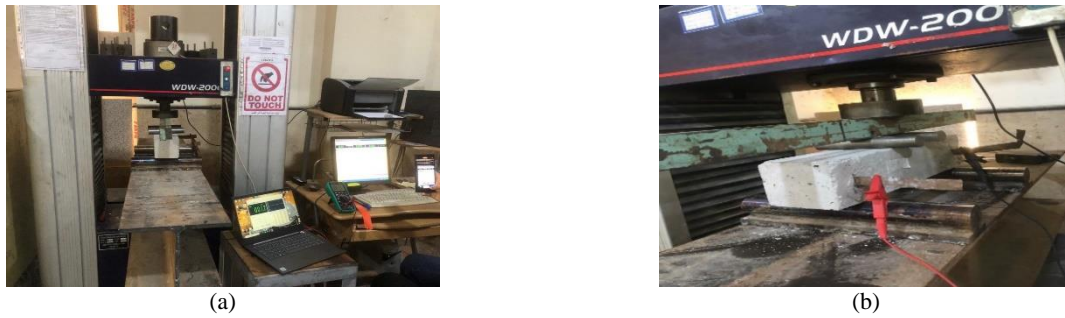


**Figure 18.** The flexural and self-sensing tests setup. (a) The flexural testing machine, (b) The prismatic specimen under loading, with capturing of the electrical resistance

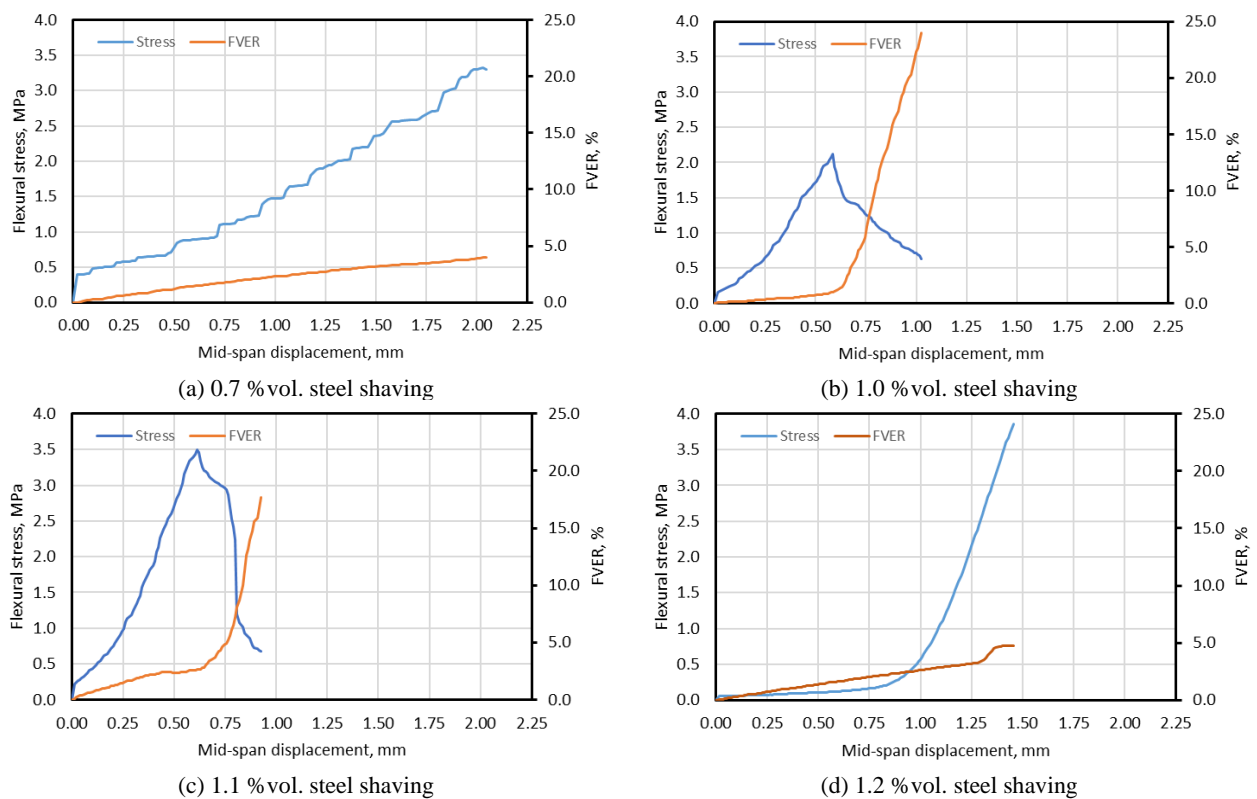


**Figure 19.** Piezoresistive behavior of prismatic specimens with different percentages of steel shavings under flexural load

of a particular little fracture that ultimately results in complete failure. With increasing bending loads and deformation experience, the FVER values show a steady increase. All blends are included, regardless of steel shaving content percentage. Deterioration, or disintegration of the conductive paths has occurred as a result of microcracks. The FVER showed a steady rise throughout the first loading segment, followed by more dramatic rises as the bending loads approach the final breaking point. This is likely caused by increased cracks (12, 14, 45-47).

In terms of ductile concrete, the mixtures containing 0.7 vol.% of steel shavings exhibit the best behavior. This behavior is due to the clear effect of steel shaving fibers

that award the concrete mixture the ductile behavior in addition to uniform changes in the electrical resistance, which means that the produced mixtures have the ability to sense the load application, damage and displacement of the prismatic specimens. Sudden failures that are happened after around 1 mm of displacement are also captured by the produced mixtures that have 1.0 and 1.1 vol.% of steel shaving fibers. At 1.2 vol.% of steel shaving fibers dosage, the prismatic specimens appeared a steadier behavior in terms of flexural strength and the resulted mid-span displacement with a successful self-sensing behavior. In essence, the rising of FVER with the progression of the flexural load application is due to the fracture induces the dispersion of concrete particles,



resulting in the formation of wider gaps or voids between them. The expanded gaps impede the movement of electrons, resulting in a rise in the electrical resistivity even when the material is experiencing failure (44, 48-51).

Nevertheless, the dispersion and divergence of particles disturb the networks through which electricity flows in the material, resulting in an elevation of the electrical resistance. Comprehending this behavior is vital for interpreting the electrical reaction of materials when subjected to stress and failure circumstances, especially in situations where it is necessary to self-detect or monitor the structural health through electrical properties.

## 7. CONCLUSIONS

A comprehensive research endeavor was undertaken to assess the self-sensing capabilities and mechanical attributes of concrete compositions derived from waste materials. The evaluation of mechanical properties involved testing through compressive, splitting, and flexural examinations of different concrete mixtures. The investigation of self-sensing capabilities entailed analyzing the Fractional Variation in Electrical Resistance (FVER) concerning various applied load scenarios across cubic, cylindrical and prismatic specimens. Consequently, several conclusions can be drawn from these investigations:

1. The slump test for concrete containing steel shaving compared to the base concrete shows that the id declined the increasing of the steel shaving fiber dosage
2. The specimens containing steel shaving have a higher compressive strength than the control mix (R30S1.2), and the amount of strength is increased with the increase in the amount added of steel shaving fibers
3. The addition of the steel shaving fibers to the mixtures enhances the strength ability regarding the applied indirect tension loads. This improvement is raised with the increasing of the fiber dosages. Moreover, the indirect tensile strength is improved the progression of the curing age of the mixtures
4. An enhancement was obtained in the flexural strength and this enhancement is proportional to the amount of steel shaving fibers
5. The ultrasonic pulse velocity test results proved the compressive strength results of the different mixtures produced in the present work
6. All mixture types exhibit good piezoresistive behavior regarding the loads applied on them (compression, indirect tension and bending) even with low dosages of steel shaving fibers. This behavior opens the door widely to the possibility of producing rigid pavement mixtures with good mechanical and smart properties from waste materials

## 8. REFERENCES

1. Singh B, Ishwarya G, Gupta M, Bhattacharyya S. Geopolymer concrete: A review of some recent developments. *Construction and building materials*. 2015;85:78-90. <https://doi.org/10.1016/j.conbuildmat.2015.03.036>
2. Arslan MH, Yazman Ş, Hamad AA, Aksoylu C, Özkılıç YO, Gemi L, editors. Shear strengthening of reinforced concrete T-beams with anchored and non-anchored CFRP fabrics. *Structures*; 2022: Elsevier. <https://doi.org/10.1016/j.istruc.2022.03.046>
3. Sharba AAK, Ibrahim AJ. Evaluating the use of steel scrap, waste tiles, waste paving blocks and silica fume in flexural behavior of concrete. *Innovative Infrastructure Solutions*. 2020;5(3):94. <https://doi.org/10.1007/s41062-020-00341-8>
4. Abbas A. Management of steel solid waste generated from lathes as fiber reinforced concrete. *Eur J Sci Res*. 2011;50(4):481-5.
5. Wang X, Fan F, Lai J, Xie Y, editors. Steel fiber reinforced concrete: A review of its material properties and usage in tunnel lining. *Structures*; 2021: Elsevier. <https://doi.org/10.1016/j.istruc.2021.07.086>
6. Mansi AH, Galal OH, Lafi M, editors. The utilisation of lathe steel waste fibers to improve plain concrete. *Proceedings of the Ninth International Conference on Advances in Civil, Structural and Mechanical Engineering*, Rome, Italy; 2019. 10.15224/978-1-63248-182-5-05
7. Annadurai A, Ravichandran A. Seismic behavior of beam-column joint using hybrid fiber reinforced high-strength concrete. *Iranian Journal of Science and Technology, Transactions of Civil Engineering*. 2018;42(3):275-86. <https://doi.org/10.1007/S40996-018-0100-9>
8. Akshaya T, Manikandan G, Baby JE, Jaambavi I. WITHDRAWN: Experimental study on bending behaviour of fibre reinforced concrete by using lathe waste fiber. Elsevier; 2021.
9. Hicks RG. Alaska soil stabilization design guide. Alaska. Department of Transportation and Public Facilities. Research and ...; 2002.
10. Al-Dahawi A, Yıldırım G, Öztürk O, Şahmaran M. Assessment of self-sensing capability of Engineered Cementitious Composites within the elastic and plastic ranges of cyclic flexural loading. *Construction and Building Materials*. 2017;145:1-10. <https://doi.org/10.1016/j.conbuildmat.2017.03.236>
11. Al-Dahawi AM. Effect of curing age on the self-sensing behavior of carbon-based engineered cementitious composites (ECC) under monotonic flexural loading scenario. *MATEC Web of Conferences*. 2018;162. 10.1051/mateconf/201816201034
12. Sarwary MH, Yıldırım G, Al-Dahawi A, Anil O, Khiavi KA, TOKLU K, et al. Self-Sensing of Flexural Damage in Large-Scale Steel-Reinforced Mortar Beams. *ACI Materials Journal*. 2019;116(4):209-21. 10.14359/51715581
13. Hameed IT, Al-Dahawi A. Electro-mechanical Properties of Functional Fiber-Based Rigid Pavement under Various Loads Applied on a Large-Scale in-Situ Section. *E3S Web of Conferences*. 2023;427:03033. <https://doi.org/10.1051/e3sconf/202342703033>
14. Yıldırım G, Sarwary MH, Al-Dahawi A, Öztürk O, Anil Ö, Şahmaran M. Piezoresistive behavior of CF- and CNT-based reinforced concrete beams subjected to static flexural loading: Shear failure investigation. *Construction and Building Materials*. 2018;168:266-79. 10.1016/j.conbuildmat.2018.02.124
15. Mussa F, Al-Dahawi A, Banyhussan QS, Baanoon MR, Shalash MA. Carbon Fiber-Reinforced Asphalt Concrete: An Investigation of Some Electrical and Mechanical Properties. *IOP Conference Series: Materials Science and Engineering*. 2020;737:012122. 10.1088/1757-899X/737/1/012122

16. Raid D, Abdullah AA-D, Hussein H, Zghair. Mechanical Characteristics and Self-Monitoring Technique of Smart Cementitious Mixtures with Carbon Fiber and Graphite Powder as Hybrid Functional Additives. *Engineering and Technology Journal*. 2022;40(11):1-11. <http://doi.org/10.30684/etj.2022.134097.1220>
17. Raid D, Abdullah AA-D, Hussein H, Zghair. Mechanical and self-sensing properties of cementitious composites with hybrid carbon particles/fibers as functional fillers. *AIP Conference Proceedings*. 2023;2830(1):030017. <https://doi.org/10.1063/5.0156827>
18. Ayad K, Mohammed AMA-D, Qais S, Banyhussan. Effect of adding additional Carbon Fiber on Piezoresistive Properties of Fiber Reinforced Concrete Pavements under Impact Load. *Engineering and Technology Journal*. 2021;39(12):1771-80. <http://doi.org/10.30684/etj.v39i12.1942>
19. Dong W, Li W, Tao Z, Wang K. Piezoresistive properties of cement-based sensors: Review and perspective. *Construction and Building Materials*. 2019;203:146-63. [10.1016/j.conbuildmat.2019.01.081](https://doi.org/10.1016/j.conbuildmat.2019.01.081)
20. Baranek S, Cerny V, Drochytka R, Meszarosova L, Melichar J. Electrically conductive composite materials with incorporated waste and secondary raw materials. *Scientific Reports*. 2023;13(1):9023. <https://doi.org/10.1038/s41598-023-36287-x>
21. Piro NS, Mohammed AS, Hamad SMJJoSM. Evaluate and predict the resist electric current and compressive strength of concrete modified with GGBS and steelmaking slag using mathematical models. 2023;9(1):194-215. <https://doi.org/10.1007/s40831-022-00631-8>
22. Çelik Aİ, Özkılıç YO, Zeybek Ö, Özdöner N, Tayeh BA. Performance Assessment of Fiber-Reinforced Concrete Produced with Waste Lathe Fibers. 2022;14(19):11817. <https://doi.org/10.3390/su141911817>
23. Yadav N, Kumar R. Performance and Economic Analysis of the Utilization of Construction and Demolition Waste as Recycled Concrete Aggregates. *International Journal of Engineering*. 2024;37(3):460-7. [10.5829/ije.2024.37.03c.02](https://doi.org/10.5829/ije.2024.37.03c.02)
24. AASHTO-T27. Standard Method of Test for Sieve Analysis of Fine and Coarse Aggregates. USA: AASHTO; 1993. p. 4.
25. Banyhussan QS, Hanoon AN, Al-Dahawi A, Yıldırım G, Abdulhameed AA. Development of gravitational search algorithm model for predicting packing density of cementitious pastes. *Journal of Building Engineering*. 2020;27. [10.1016/j.jobe.2019.100946](https://doi.org/10.1016/j.jobe.2019.100946)
26. Afrawee ARM, Aodah HH, Mohammed HA, editors. Development of the Iraqi highways management system-Case study: Basrah–Nasiriyah’s highway. *AIP Conference Proceedings*; 2020: AIP Publishing. <https://doi.org/10.1063/5.0030802>
27. Güneyisi E, Gesoğlu M, Karaoğlu S, Mermerdaş K. Strength, permeability and shrinkage cracking of silica fume and metakaolin concretes. *Construction and Building Materials*. 2012;34:120-30. <https://doi.org/10.1016/j.conbuildmat.2012.02.017>
28. SCR. State Commission of Roads and Bridges, Standard specifications for Roads and Bridges. Iraq: Ministry of Construction, Housing, Municipalities and Public Works, Department of Planning and Studies; 2003.
29. Taylor HF. *Cement chemistry*: Thomas Telford London; 1997.
30. Al-Hindawi LAA, Al-Dahawi AM, Al-Zuheriy ASJ. Use of Waste Materials for Sustainable Development of Rigid Pavement. *International Journal of Engineering*. 2023;36(10):13. [10.5829/ije.2023.36.10a.16](https://doi.org/10.5829/ije.2023.36.10a.16)
31. BS-EN-12390-6. Testing hardened concrete—Tensile splitting strength of test specimens. 2009. p. 14.
32. ASTM-C496/C496M. Standard Test Method for Splitting Tensile Strength of Cylindrical Concrete Specimens. US: ASTM International; 2011. p. 5.
33. ASTM-C78. Standard test method for flexural strength of concrete (using simple beam with third-point loading). *Annual book of ASTM standards*2002. p. 3.
34. Al-Dahawi A, Sarwary MH, Öztürk O, Yıldırım G, Akın A, Şahmaran M, et al. Electrical percolation threshold of cementitious composites possessing self-sensing functionality incorporating different carbon-based materials. *Smart Materials and Structures*. 2016;25(10):1-15. <http://dx.doi.org/10.1088/0964-1726/25/10/105005>
35. Junaid M, Shah MZA, Yaseen G, Awan HH, Khan D, Jawad M. Investigating the Effect of Gradation, Temperature and Loading Duration on the Resilient Modulus of Asphalt Concrete. *Civil Engineering Journal*. 2022;8(02). <http://dx.doi.org/10.28991/CEJ-2022-08-02-07>
36. Balamuralikrishnan R, Saravanan J. Effect of addition of alccofine on the compressive strength of cement mortar cubes. *Emerging Science Journal*. 2021;5(2):155-70. <https://doi.org/10.28991/esj-2021-01265>
37. Mohana MH. Assessment of concrete compressive strength by ultrasonic pulse velocity test. *Iraqi Journal of Civil Engineering*. 2020;14(1):39-46. DOI: 10.37650/ijce.2020.172874
38. Elvery R, Ibrahim L. Ultrasonic assessment of concrete strength at early ages. *Magazine of Concrete Research*. 1976;28(97):181-90. <https://doi.org/10.1680/mac.1976.28.97.181>
39. Manaswini C, Vasu D. Fibre Reinforced Concrete from Industrial Waste-A Review. *International Journal of Innovative Research in Science, Engineering and Technology*. 2015;4(12):11751-8. [:10.15680/IJIRSET.2015.0412013](https://doi.org/10.15680/IJIRSET.2015.0412013)
40. Aksoyulu C, Yazman Ş, Özkılıç YO, Gemi L, Arslan MH. Experimental analysis of reinforced concrete shear deficient beams with circular web openings strengthened by CFRP composite. *Composite Structures*. 2020;249:112561. <https://doi.org/10.1016/j.compstruct.2020.112561>
41. Shewalul YW. Experimental study of the effect of waste steel scrap as reinforcing material on the mechanical properties of concrete. *Case Studies in Construction Materials*. 2021;14:e00490. <https://doi.org/10.1016/j.cscm.2021.e00490>
42. Prasad BP, Maanvit PS, Jagarapu DCK, Eluru A. Flexural behavior of fiber reinforced concrete incorporation with lathe steel scrap. *Materials Today: Proceedings*. 2020;33:196-200. <https://doi.org/10.1016/j.matpr.2020.03.793>
43. British Standards Institution (BSI): London U. 12504-4: 2021; *Testing Concrete in Structures—Determination of Ultrasonic Pulse Velocity*. 2021.
44. Ghadhbani D, Joni HH, Al-Dahawi AM. Carbon Fiber-Based Cementitious Composites for Traffic Detection and Weighing In Motion. *Engineering and Technology Journal*. 2021;39(8):1250-6. [10.30684/etj.v39i8.1875](https://doi.org/10.30684/etj.v39i8.1875)
45. Yıldırım G, Öztürk O, Al-Dahawi A, Ulu AA, Şahmaran M. Self-sensing capability of Engineered Cementitious Composites: Effects of aging and loading conditions. *Construction and Building Materials*. 2020;231:117-32. <https://doi.org/10.1016/j.conbuildmat.2019.117132>
46. Katsaga T. Geophysical imaging and numerical modelling of fractures in concrete 2010.
47. Rohith Sai K, Girija Sravani K, Srinivasa Rao K, Balaji B, Agarwal V. Design and Performance Analysis of High-k Gate All Around Fin-field Effect Transistor. *International Journal of Engineering*. 2024;37(3):476-83. [10.5829/ije.2024.37.03c.04](https://doi.org/10.5829/ije.2024.37.03c.04)
48. Al-Attar TS, Al-Zuheriy ASJ, Hamza SM. Optimum Steel Fiber Content of High Strength Pozzolime Concrete %J *Engineering and Technology Journal*. 2021;39(12):1869-74. [10.30684/etj.v39i12.2213](https://doi.org/10.30684/etj.v39i12.2213)

49. Sunarsih ES, As' ad S, Sam ARM, Kristiawan SA. Properties of Fly Ash-Slag-Based Geopolymer Concrete with Low Molarity Sodium Hydroxide. *Civil Engineering Journal*. 2023;9(02):381-92. 10.28991/CEJ-2023-09-02-010
50. Amaludin AE, Asrah H, Mohamad HM, bin Amaludin HZ, bin Amaludin NA. Physicochemical and microstructural characterization of Klias Peat, Lumadan POFA, and GGBFS for geopolymer based soil stabilization. *HighTech and Innovation Journal*. 2023;4(2):327-48. 10.28991/HIJ-2023-04-02-07
51. Al-Kasassbeh S, Al-Thawabteh J, Al-Kharabsheh E, Al-Tamseh A. Influential and intellectual structure of geopolymer concrete: a bibliometric review. *Civil Engineering Journal*. 2023;9(9):2330-44. 10.28991/CEJ-2023-09-09-017

#### COPYRIGHTS

©2024 The author(s). This is an open access article distributed under the terms of the Creative Commons Attribution (CC BY 4.0), which permits unrestricted use, distribution, and reproduction in any medium, as long as the original authors and source are cited. No permission is required from the authors or the publishers.



#### Persian Abstract

##### چکیده

حمایت از توسعه پایدار، کمک به کاهش ضایعاتی که باعث آسیب های زیست محیطی می شود و کاهش استفاده از مواد طبیعی بخشی از حفظ محیط زیست و جامعه است. این امر با برجسته ساختن روسازی بتنی پایدار با کیفیت قابل قبول و بر اساس مشخصات انجام می شود. نویسندگان قبلاً با جایگزینی جزئی سیمان پرتلند با ۵۵ درصد وزنی سرباره کوره بلند دانه بندی شده زمینی (GGBFS) و همچنین جایگزینی جزئی سنگدانه های بکر با ۳۰ درصد وزنی سنگدانه بازیافتی خرد شده، مخلوطی از روسازی بتنی با خواص بهینه تولید کردند. روسازی صلب هدف از این کار تحقیقاتی تولید مخلوطی از روسازی سفت و سخت خودحسگر از ضایعات با خواص مکانیکی بالا، بهتر از بتن معمولی و کم هزینه است. مخلوط جدید جدید این توانایی را دارد که آسیب های وارده به روسازی بتنی را زودتر تشخیص دهد تا با حفظ دوره ای روسازی به موقع، عمر طولانی تری داشته باشد. مخلوط قبلی با افزودن الیاف ریش تراش فولادی خرد شده با طول های ۲۰-۶۰ میلی متر در چهار نسبت حجمی مختلف بهبود یافت. اینها ۰.۷٪، ۱٪، ۱.۱٪ و ۱.۲٪ هستند. نتایج با نتایج مخلوط پایه مقایسه شد و کاهش در کارایی و مقادیر اسلامپ مشاهده شد. علاوه بر این، بهبود قابل توجهی در خواص مکانیکی به دست آمد. مقاومت بتن در برابر بارهای وارده با افزایش درصد تراشیدن فولاد در مخلوط ها به دلیل افزایش نیروهای چسبندگی درون مخلوط افزایش یافت. قابلیت خود سنجشی برای مخلوط های توسعه یافته با اندازه گیری تغییرات مقاومت الکتریکی تحت انواع مختلف بارهای مکانیکی آزمایش شد. نتایج نشان داد که جهت بار اعمال شده و نسبت تراشه های فولادی بر خواص خودحسگر از نظر تغییرات کسری در مقاومت الکتریکی (FVER، %) تأثیر می گذارد که اهمیت استفاده از تراشه های فولادی را در تولید بتن هوشمند نشان می دهد. روسازی از منابع استفاده مجدد کارآمدتر و مقرون به صرفه تر است.